FLUIDS ASSOCIATED WITH THE CAXIAS MESOTHERMAL GOLD MINERALIZATION, SÃO LUÍS CRATON, NORTHERN BRAZIL: A FLUID INCLUSION STUDY

EVANDRO LUIZ KLEIN[1], KAZUO FUZIKAWA[2], JAIR CARLOS KOPPE[3] AND MARIA SYLVIA SILVA DANTAS[4]

ABSTRACT   The Caxias deposit is situated in the Gurupi Auriferous Province of the Paleoproterozoic São Luís Craton, northern Brazil. It is a lode-type gold mineralization associated with a narrow, steeply dipping, NE-trending, shear zone crosscutting a hydrothermalized microtonalite (northern sector) and schists (southern sector). Fluid inclusion studies on vein quartz crosscutting the microtonalite (northern sector) have identified early carbonic and aqueous-carbonic inclusions and late aqueous inclusions, unrelated to the mineralizing event. The CO_2/H_2O ratio and the other microthermometric properties show a wide range of values, which are interpreted as product of heterogeneous trapping of two (partially) immiscible fluids and to deformation-related post-formational processes. The resulting mineralizing fluid has XCO_2: 6-45 mol %; XN_2: < 2.5 mol %; XH_2O: 55-95 mol %; mean salinity of 4.5 wt % NaCl equiv., and moderate density (0.7-1.0 g/cm^3). Bulk isochores coupled with chlorite geothermometry constrained the P-T entrapment conditions between 262-307ºC and 1.6-3.7 kb. Log O_2 for this P-T-X range was estimated between –29.8 and –34.2. Geological characteristics and fluid properties found in the northern sector of Caxias gold mineralization are similar to those described for metamorphic fluids of mesothermal gold deposits.

Keywords: Gold, aqueous-carbonic fluids, mesothermal, Paleoproterozoic, São Luís Craton, Brazil

INTRODUCTION   Caxias is a small primary gold deposit located in the São Luís Craton, northern Brazil (Fig. 1), along with several others small deposits and showings. This region has been the focus of intermittent alluvial mining since the second half of 17th century. Petrographic, geochemical, geochronological and fluid inclusion studies were carried out in the Caxias and Areal deposits (Klein 1998). This paper presents a characterization of the fluids of the northern sector of the Caxias gold mineralization, based on microthermometric and Raman spectrographic studies. Genetic considerations about this Au mineralization are done as well, supported by the fluid inclusion data.

GEOLOGICAL SETTING AND CHARACTERISTICS OF THE MINERALIZATION   Three major geotectonic units are recognized in the Gurupi region (Cordani *et al.* 1968, Abreu 1990, Pastana 1995): a stable area, a mobile zone, and sedimentary covers (Fig. 1). The stable area corresponds to the Paleoproterozoic São Luís Craton (**SLC**). It is bordered by the Neoproterozoic Gurupi Shear Belt. Proterozoic and phanerozoic sedimentary basins cover the former geotectonic units. The **SLC** comprises dominant granitoids of the Tromaí Suite and minor supracrustal rocks from the Aurizona Group. The metaluminous, calc-alkaline Tromaí granitoids have trace elements patterns comparable with modern, subduction-related, volcanic arc granites (Pastana 1995, Klein 1998).

The Caxias gold mineralization occurs on two different host rocks (Klein 1998): in the northern sector (N-CX) the mineralization is hosted by a small intrusion of a fine-grained tonalite, with strong chloritic (+ carbonate, sericite, epidote, pyrite, sphalerite) alteration; in the southern sector (S-CX) the host-rocks are quartz-sericite- and biotite-chlorite-schists from the Aurizona Group (Fig. 2), with pyrite dissemination. In both areas, mineralization is spatially related to a steeply-dipping, meter wide, N15-25E-trending, dextral, transcurrent shear zone. Gold occurs disseminated in the hydrothermally altered rocks and in crosscutting quartz veinlets, especially at the contact of quartz and chlorite grains.

FLUID INCLUSION STUDY   This paper presents the fluid inclusion (**FI**) data from the northern sector of the Caxias mineralization. Quartz is largely the dominant mineral phase in the veinlets (> 90% vol.), which also contain pyrite, carbonate and chlorite. Quartz grains are xenomorphic, limpid and range from 0,4 to 2 mm in size. Slight to moderate undulatory extinction, localized mortar texture, and deformation lamellae are observed, suggesting weak ductile deformational processes.

Sample preparation and microthermometric measurements were carried out following the procedures outlined by Roedder (1984) and Shepherd *et al.* (1985). Microthermometry was performed with Chaixmeca heating-freezing stages in the fluid inclusion laboratories at the Universidade Federal do Rio Grande do Sul and Universidade Federal do Pará. Raman analyses were performed at the Universidade Federal de Minas Gerais on a Dilor Raman microprobe with a multichannel detector and the 514,53-nm line of an Ar laser. Instrumental settings were kept constant during the analyses.

Fluid inclusion description and classification   Based on relative phase proportions in the fluid inclusions at room and subzero temperatures, three types of fluid inclusions have been identified.

Type I One-phase carbonic (CO_2) fluid inclusions are clear to dark, mainly irregular in shape and their sizes vary between 6 and 30 mm. Small proportions (< 10%) of petrographically and microthermometrically undetectable H_2O may be admitted in these inclusions. They are the least frequent of all three types and are randomly distributed in the transparent domains of the host quartz. Most of the time they are associated with type II inclusions (Fig. 3); few are isolated and they are seldom seen in the same domain with type III inclusions.

Type II H_2O-CO_2 liquid inclusions are the dominant type averaging 13 μm in size. Most inclusions are two-phased at room temperature, and may nucleate a third phase (vapor CO_2) on cooling. The volumetric proportion of the CO_2-rich phase was optically estimated, varying from 15 to 75%. They present random distribution, often clustered and coexisting with the type I inclusions (Fig. 3), and are rarely associated with type III FI.

Type III are two-phase aqueous (H_2O liquid + vapor) fluid inclusions, having characteristic clear appearance with sizes ranging from 5 to 27 μm and shapes varying from irregular to rounded or ellipsoidal. Rare daughter minerals have been observed and the degree of filling is constant (0.90-0.95). Most of the inclusions are confined to healed fractures, sharp trails and three-dimensional arrays. Only few of them occur isolated or associated with type II fluid inclusions.

Microthermometry   *TYPE I AND II FLUID INCLUSIONS* Low-temperature measurements indicated most of the carbonic phase melting temperature ($TmCO_2$) close to the CO_2 triple point (-56.6ºC), and the remaining varying down to –57.5ºC. The homogenization of the carbonic phase ($ThCO_2$) occurs always to liquid, between –3.2 and 27.7ºC and 7.9 and 30.9ºC for types I and II, respectively (Fig. 4a), corresponding to bulk densities between 0.7 and 1.0 g/cm^3. This wide spectrum of $ThCO_2$ occurs not only in different domains of the host

1   CPRM (Serviço Geológico do Brasil) – Av. Dr. Freitas, 3645, Bairro do Marco, CEP: 66095-110, Belém-PA, Brasil. Tel: 0XX 91 276.8577 – Fax: 0XX 91 276.4020 – e-mail: eklein@amazon.com.br (corresponding author)

2   CDTN/CNEN – Rua Mário Werneck, s/n, Pampulha, CEP: 31270-010, Belo Horizonte-MG, Brasil. Tel: 0XX 31 499.3140 – Fax: 0XX 31 499.3390 – e-mail: kazuo@urano.cdtn.br

3   UFRGS - Av. Osvaldo Aranha, 99/504, CEP: 90035-190, Porto Alegre-RS, Brasil. Tel: 0XX 51 316.3357 – Fax: 0XX 51 316.3394 - e-mail: jkoppe@lapes.ufrgs.br

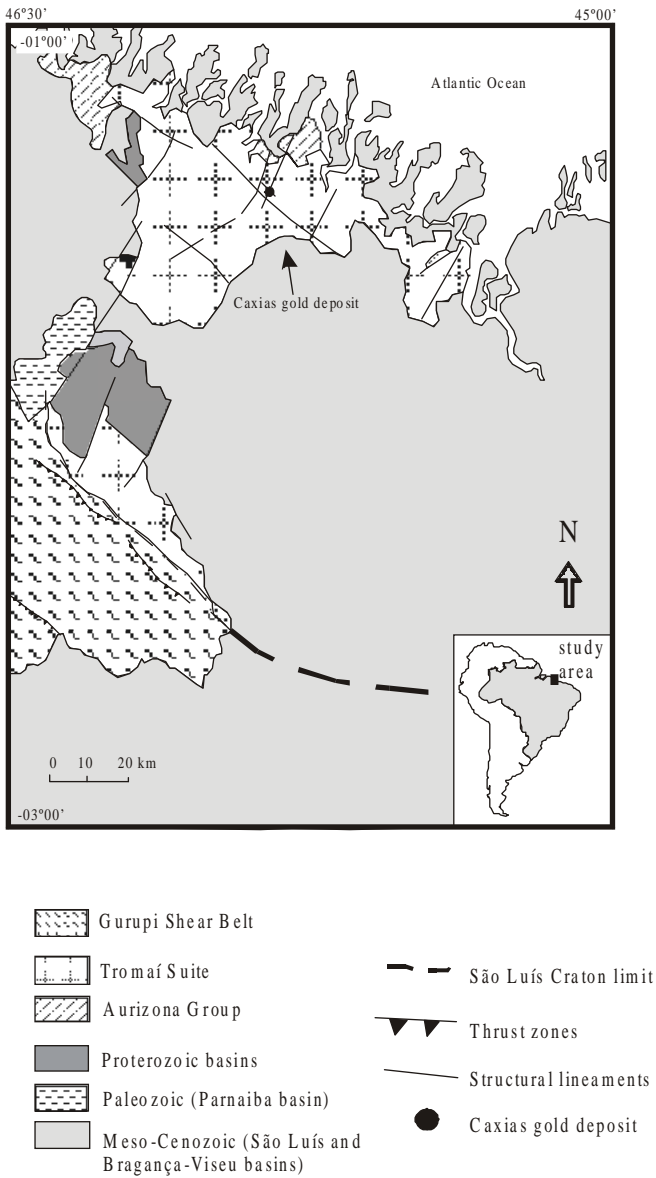4   UFMG, Departamento de Física – Av. Pres. Antonio Carlos, 6627, CEP: 31270-010, Belo Horizonte, MG.

Figure 1–Simplified geological map of the Gurupi region. Adapted from Pastana (1995).

Figure 2–Geological sketch map of the Caxias deposit. Modified from Klein (1998).

quartz but also in single clusters (Fig. 3). In type II inclusions, clathrate melting temperatures (Tmclath) always occur below the $ThCO_2$, showing little variation, with mean and mode around 7.5ºC (Fig. 4b). The total homogenization (Tht) also shows a wide range (Fig. 4c), between 205 and 378ºC.

TYPE III FLUID INCLUSIONS   Four eutectic temperatures (Te) were obtained, two around –45ºC and the two other around –27ºC. The former belongs to inclusions that show ice final melting temperature (Tmice) between –5ºC to –10ºC (salinities between 7.8 and 13.9 wt. % NaCl equiv.), and final homogenization between 180ºC and 242ºC. The second group shows Tmice in the range –0.1ºC to –7.4ºC (0.18 to 11 wt. % NaCl equiv.) and Tht ranging from 124ºC to 228ºC (Fig. 5).

Raman spectroscopy   The clustering of $TmCO_2$ around –56.6ºC, with little deviation from its triple point, suggests that the composition of carbonic phase present in types I and II fluid inclusions can be roughly considered as pure CO_2. Notwithstanding, four fluid inclusions were selected for Raman spectroscopy. Although CO_2, N_2, CH_4 and H_2S have been tested, only CO_2 and N_2 were detected. Molar proportions of these two components were calculated using the *relative Raman scattering cross-section* of 1.21 for CO_2 (N_2=1), showing N_2 mostly as traces in the carbonic phase, reaching 5 mole %
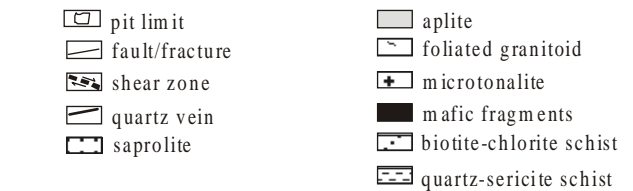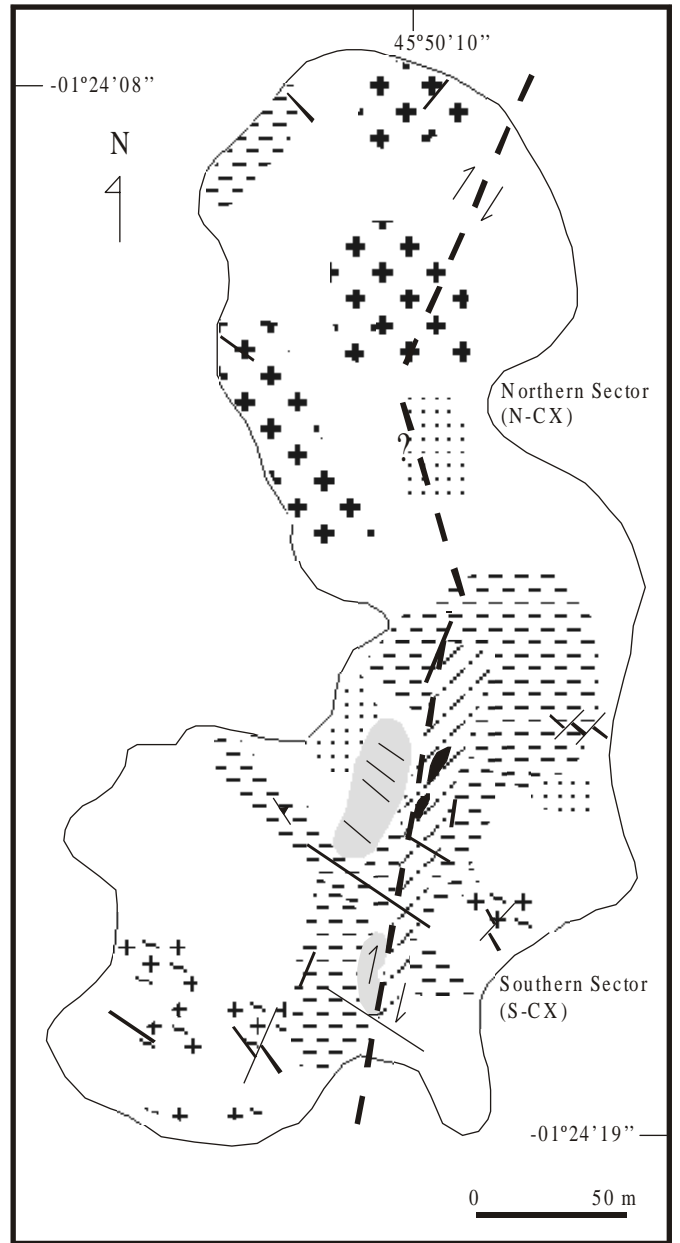
only in one FI. These results are consistent with the microthermometric data obtained using the experimental CO_2-N_2 system phase diagram of Kerkhof and Thiery (1994).

DISCUSSION AND CONCLUSIONS   The dominant group of CO_2-bearing fluid inclusions (types I and II) is considered the most precocious, and may represent primary FI. Constraints in bulk properties of these two types of CO_2-bearing fluids (P-T-V-X-fO_2) were given by combined microthermometric and Raman microspectrometric data. The composition was estimated according to
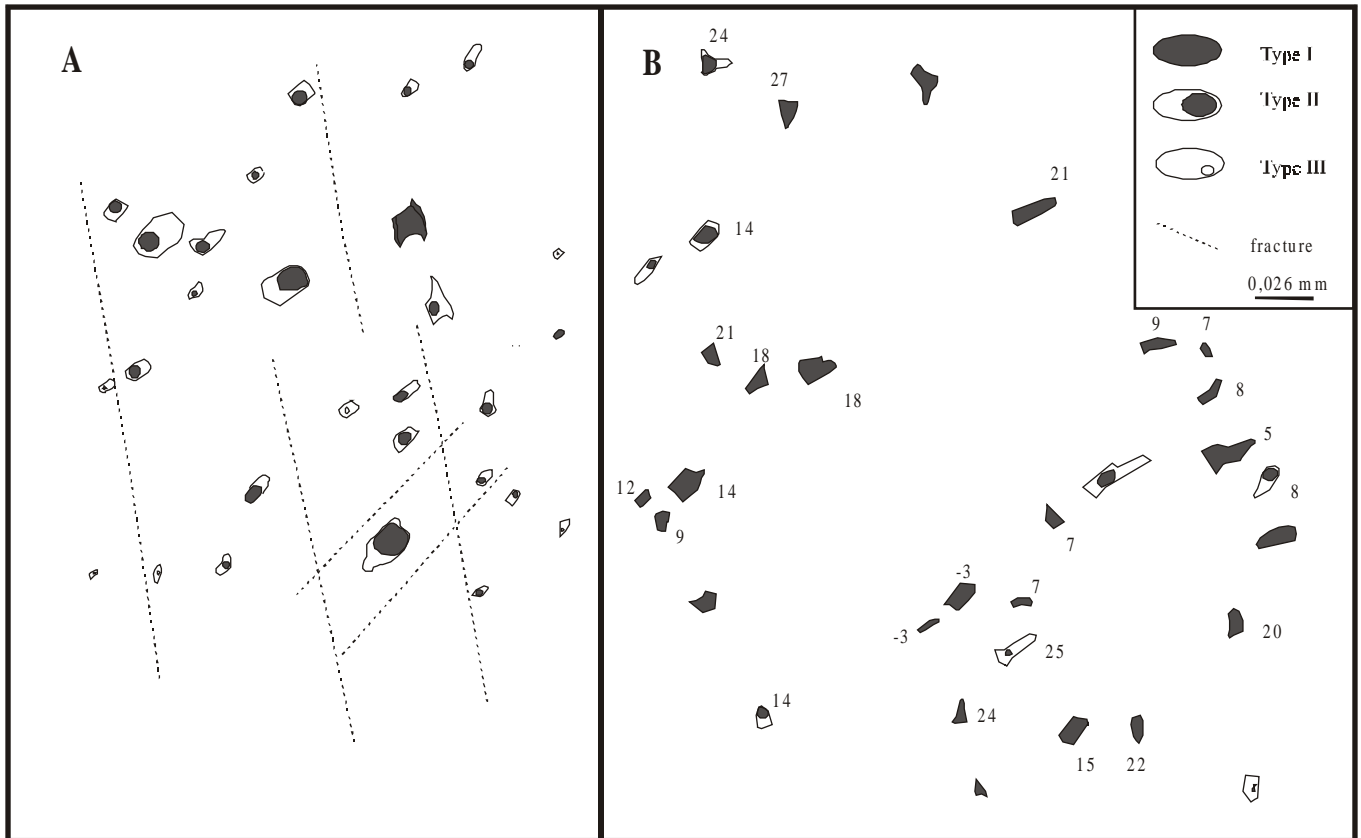
Figure 3–Distribution of types I and II fluid inclusions in the N-Caxias deposit, showing variable CO_2/H_2O phase ratios (A and B) and CO_2 homogenization temperature (B). Type III inclusions are late (see text for explanation).

Ramboz *et al.* (1985) or Holloway (1981), when the molar fraction of CO_2 in the carbonic phase is 100%. For type I fluid inclusions the presence of 5% H_2O, undetected by common petrography and microthermometry, and absence of salts have been assumed. The resulting bulk composition of the types I and II FI is XH_2O: 55 to 95 mol %, XCO_2: 6 to 45 mol %, XN_2: 0 to 2 mol %. Salinities, derived from Tmclath in type II FI, are in the 0.2 to 9.8 wt. % NaCl equiv. range, with a strong mode in 5% (mean 4.5%). Bulk densities, obtained from $ThCO_2$, are in the range 0.761 to 1.006 g/cm^3. This compositional range is compatible with metamorphic fluids produced by dehydration and decarbonization of greenstone sequences.

Type II fluid inclusions show highly variable $ThCO_2$ and Tht. This behavior may result from leakage related to heating (Shepherd *et al.* 1985), deformation (Wilkins and Barkas 1978), entrapment under pressure fluctuation (Robert and Kelly 1987), or fluid immiscibility (Ramboz *et al.* 1982). The highly variable CO_2/H_2O ratios have been used as evidence of phase separation and heterogeneous trapping (Ramboz *et al.* 1982), fluid mixing (Cassidy and Bennett 1993), or H_2O loss (Crawford and Hollister 1986). The coexistence of chemically and physically contrasting fluids (in this study, the carbonic and aqueous-carbonic FI) is an evidence that they are cogenetic and contemporaneous. This characteristic has been also attributed to successive mixing of different fluids (Pichavant *et al.* 1982), heterogeneous trapping (Ramboz *et al.* 1982), and post-entrapment modifications with variable loss of H_2O (Crawford and Hollister 1986).

Although some post-entrapment modification may have affected the CO_2-bearing FI, as evidenced by the weak ductile deformation in host quartz, this was not the dominant process that led these populations of FI to acquire the described characteristics. Besides, it is not evident in the salinity x Tht diagram for types II end III FI (Fig. 6) the vertical tendencies that are typical of necking-down and leakage by heating. Therefore, it is considered that the features presented by these fluid inclusions are characteristic of an immiscible or heterogeneous state, which may be attained by opposite processes such as mixing and unmixing (phase separation). Considering the characteristics and fluid

properties displayed by the CO_2-bearing FI, the criteria of Ramboz *et al.* (1982) for fluid immiscibility, and the close distribution between the two FI types, the inclusions may be considered as cogenetic. Therefore, the contemporaneous and heterogeneous trapping requirements are satisfied. Regarding the homogenization, the type II inclusion homogenize all to H_2O, while the final homogenization of the type I inclusions could not be detected. But, as this type I FI is CO_2-rich (estimated H_2O volume % is only 5 %) and as no bubble shrinking was observed, it must be supposed that the homogenization occurred to liquid CO_2. These features, besides the lack of a compositional continuum (Tht versus % NaCl correlation; Fig. 6) suggest that the immiscible state was probably attained by phase separation, although a mixing process cannot be totally discarded.

Type III (aqueous) FI show two different eutectic temperatures, reflecting compositional differences. The assemblage with the lowest Te is Ca-rich (±NaCl, ±$MgCl_2$) and has no association with the CO_2-bearing inclusions. The group with Te around –27°C is Na-rich (±KCl), is seldom associated with types I and II and has salinities in the same range of the type II FI. Although the Na-rich FI could be regarded as part of the phase separation process, their much lower Tht, their rather constant phase proportions, and the fact that they are mostly confined to healed fractures preclude this hypothesis. Thus the origin of this fluid, as well as the Ca-rich fluid, is ascribed to a later fluid infiltration event.

As the heterogeneous trapping of immiscible or partially immiscible fluids was suggested, the isochores intersection method (Roedder and Bodnar 1980) could be used for temperature and pressure determination of fluid entrapment. However, this procedure requires density contrasts to produce isochores with different and intersecting slopes, which is not the case here, where type I and II FI have similar density ranges. Therefore, bulk composition isochores, calculated from fluid inclusion data combined with geothermometry of hydrothermal chlorites from the host microtonalite (Klein 1998), bracketed the P-T conditions between 262°C and 307°C and 1.6 kb and 3.7 kb (Fig. 7). These conditions are compatible with crustal depths of the brittle-ductile transition and beginning of the greenschist facies metamorphism.
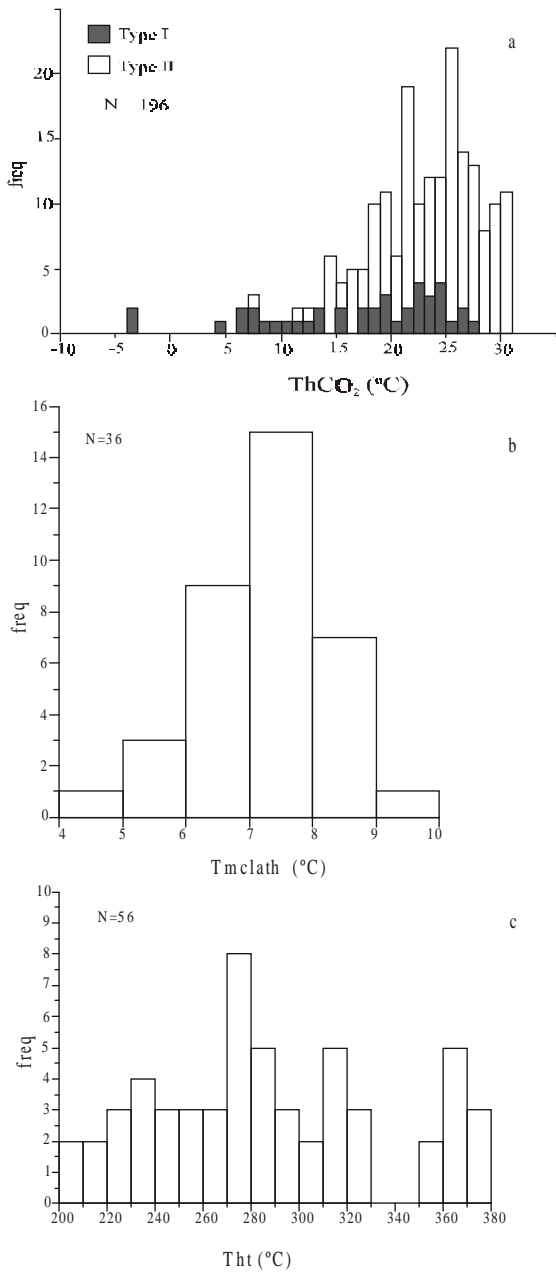
Figure 6–Salinity versus final homogenization plot for type II (triangles) and III (asterisks) fluid inclusions.

Figure 7–P-T grid for N-Caxias mineralization. Isochores labeled A and B cover the density range of type II fluid inclusions. Isochores C and D cover the density range of type I fluid inclusions. A limit of 262-307°C is given by the chlorite geothermometer. The stippled area represents the P-T conditions for the gold mineralization at N-Caxias.

Figure 4–Histograms showing microthermometric data of type I and type II fluid inclusions from N-Caxias. a: CO_2 homogenization temperature (ThCO_2); b: clathrate melting temperature for type II inclusions (Tmclath); c: total homogenization temperatures for type II inclusions (Tht).
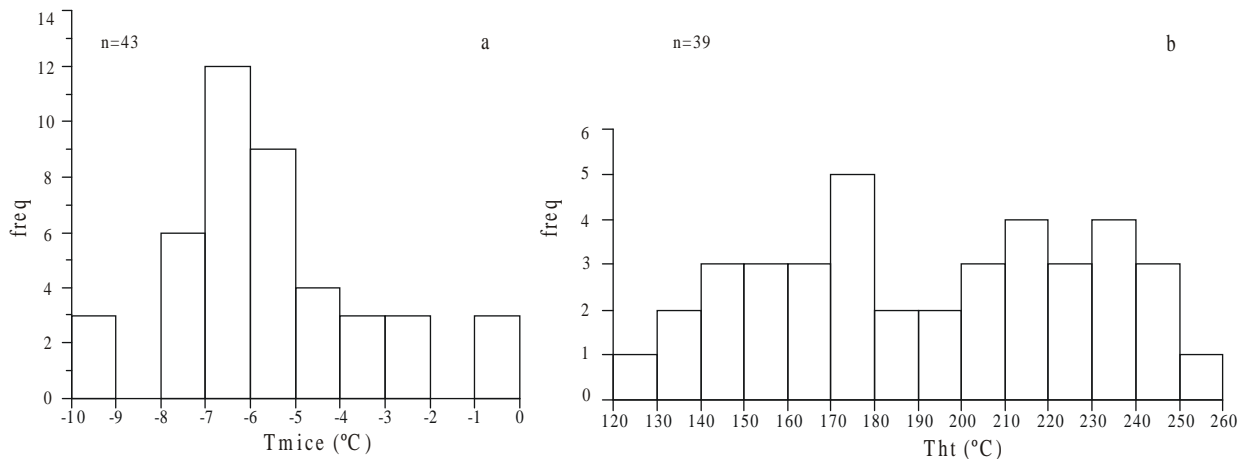

Figure 5–Histograms showing the microthermometric data of type III fluid inclusions of N-Caxias. a: ice melting temperature (Tmice); b: final homogenization temperature (Tht).
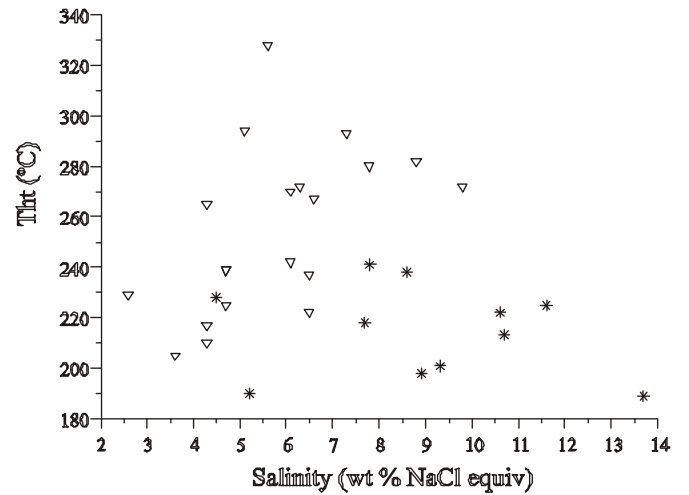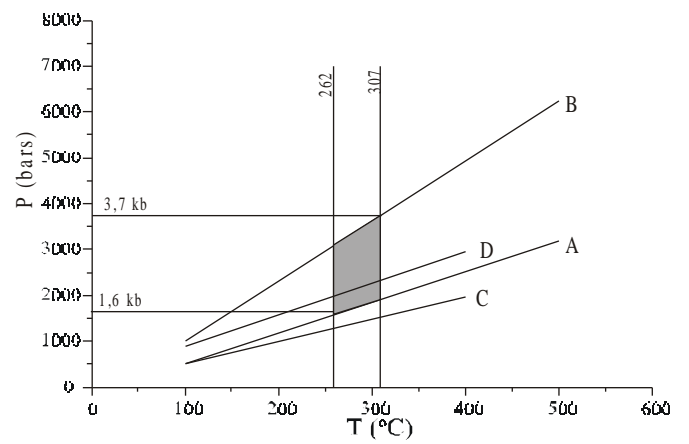
Oxygen fugacities were calculated for the P-T-X range obtained from FI data, according to the equation of Ohmoto and Kerrick (1977), considering the equilibrium $C + O_2 = CO_2$, and using the fugacity coefficient of Ryzhenko and Volkov (1971). Values of log $f O_2$ obtained through this procedure range from –29.8 to –34.2, and are similar to those reported for Archean lode-gold deposits by Groves and Foster (1991).

The last point to deal with is the source and the role of the nitrogen on the volumetric and compositional properties of the CO_2-bearing fluid inclusions. Hydrothermal alteration of K-bearing minerals, such as feldspars and micas and the breakdown of organic matter present in sediments are possible sources of N_2 (Kreulen and Schuiling 1982,

Andersen *et al.* 1993). As the concentration of N_2 is low, the only noticed influence was a small lowering of the carbonic phase melting temperature, while no relationship of its presence and the CO_2 density ($ThCO_2$) was observed.

Concluding, the geological setting, mineralogy, structural style, besides P-T-X-$f O_2$ characteristics derived from fluid inclusions, suggest that this low-salinity, reduced, aqueous-carbonic fluid, responsible for the gold mineralization in the northern sector of the Caxias deposit, is similar to the ore-bearing metamorphic fluids postulated for mesothermal gold mineralization hosted by shear zones and granite-greenstone sequences in several Precambrian cratons worldwide.

References

Abreu F.A.M. de 1990. *Evolução geotectônica do Pré-Cambriano da região Meio Norte do Brasil e sua correlação com a África Ocidental.* Curso de Pós Graduação em Geociências, Universidade Federal do Pará, Ph.D. Thesis, 440 p.

Andersen T., Austrheim H., Burke E.A.J., Elvevold, S. 1993. N_2 and CO_2 in deep crustal fluids: evidence from the Caledonides of Norway. *Chemical Geology*, **108**:113-132.

Cassidy K.F. & Bennett J.M. 1993. Gold mineralisation at the Lady Bountiful Mine, Western Australia: an example of a granitoid hosted Archaean lode gold deposit. *Mineralium Deposita*, **28**:388-408.

Cordani U.G., Melcher G.C., Almeida F.F.M. de 1968. Outline of the Precambrian geochronology of South America. *Canadian Journal of Earth Sciences*, **5**:629-632.

Crawford M.L. & Hollister L.S. 1986. Metamorphic fluids: the evidence from fluid inclusions. In: J.V. Walther & B.J. Wood (eds) *Fluid rock interaction during metamorphism*. Physical Geochemistry, Berlin, Heidelberg, New York, Springer, **5**:1-35.

Groves D.I. & Foster R.P. 1991. Archean lode gold deposits. In: R.P. Foster (ed.) *Gold metallogeny and exploration*. Glasgow, Blackie & Son, 63-103.

Holloway J.R. 1981. Composition and volumes of supercritical fluids in the Earth crust. In: L.S. Hollister & M.L. Crawford (eds.) *Fluid inclusions: applications to petrology*. Mineralogical Assoc. of Canada, Short Course Handbook, **6**:13-38.

Kerkhof F. van den, Thiéry R. 1994. Phase transitions and density calculation in the CO_2-CH_4-N_2 system. In: B. De Vivo & M.L. Frezzotti (eds.) *Fluid inclusions in minerals: methods and applications*. Blacksburg, Virginia Tech, 171-190.

Klein E. L. 1998. *Aspectos geoquímicos, geocronológicos e estudo dos fluidos associados às mineralizações auríferas dos garimpos Caxias e Areal, Cráton de São Luís, Noroeste do Maranhão*. Instituto de Geociências, Universidade Federal do Rio Grande do Sul, M. Sc. Thesis, 189 p.

Kreulen R. & Schuiling R.D. 1982. N_2-CH_4-CO_2 fluids during formation of the Dôme de l'Agout, France. *Geochimica et Cosmochimica Acta*, **46**:193-203.

Ohmoto H. & Kerrick D. 1977. Devolatilization equilibria in graphitic systems. *American Journal of Science*, **277**:1013-1044.

Pastana J.M. do N. (org.) 1995. *Programa Levantamentos Geológicos Básicos do Brasil.* Programa Grande Carajás. Turiaçu/Pinheiro, folhas SA.23-V-D/SA.23-Y-B. Estados do Pará e Maranhão. Brasília, CPRM, 205 p.

Pichavant M., Ramboz C., Weisbrod A. 1982. Fluid immiscibility in natural processes: use and misuse of fluid inclusion data. I. Phase equilibria analysis – A theoretical and geometrical approach. *Chemical Geology*, **37:**1-27.

Ramboz C., Pichavant M., Weisbrod A. 1982. Fluid immiscibility in natural pro_esses: Use and misuse of fluid inclusion data. II. Interpretation of fluid inclusion data in terms of immiscibility. *Chemical Geology*, **37**:29-48.

Ramboz C., Schnapper D., Dubessy J. 1985. The P-V-T-X-fO_2 evolution of H_2O-CO_2-CH_4-bearing fluid in a wolframite vein: reconstruction from fluid inclusion studies. *Geochimica et Cosmochimica Acta*, **49**:205-219.

Robert F. & Kelly W.C. 1987. Ore-forming fluids in Archean gold-bearing quartz veins at the Sigma Mine, Abitibi greenstone belt, Quebec, Canada. *Economic Geology*, **82**:1464-1482.

Roedder E. 1984. *Fluid Inclusions*. Mineral Soc of America. Reviews in Mineralogy, **12**:644 p.

Roedder E. & Bodnar R.J. 1980. Geologic pressure determinations from fluid inclusion studies. *Annual Reviews in Earth and Planetary Sciences*, **8**:263-301.

Ryzhenko B.N. & Volkov V.P. 1971. Fugacity coefficients of some gases in a broad range of temperature and pressures. *Geochimica International*, **8**:468-481.

Shepherd T.J., Rankin A.H., Alderton D.H. 1985. *A practical guide to fluid inclusion studies*. Glasgow, Blackie and Son, 239 p.

Wilkins R.W.T. & Barkas J.P. 1978. Fluid inclusions, deformation and recrystallization in granite tectonites. *Contributions to Mineralalogy and Petrology*, **65**:293-299.